TITLE PAGE

Title: Removal of inhibition uncovers latent movement preparation dynamics

Abbreviated title: Motor potential during saccade preparation

Authors: Uday K. Jagadisan[1,3] and Neeraj J. Gandhi[1,2,3]

Author affiliations:
[1]Department of Bioengineering
[2]Department of Neuroscience
[3]Center for the Neural Basis of Cognition
University of Pittsburgh, Pittsburgh, PA 15213

Corresponding author: Uday K. Jagadisan, Ph.D.
153 Eye and Ear Institute
203 Lothrop St
Pittsburgh, PA 15213
USA
Tel: +1-315-4099934
E-mail: kj.udayakiran@gmail.com

Author Contributions: U.K.J and N.J.G designed the study. U.K.J. performed the experiments and analyzed the data. U.K.J and N.J.G wrote the manuscript.

Number of pages: 40

Number of figures: 7 + 2 supplementary figures

Number of words: Abstract - 209, Main text - 5859, Methods - 2144

Conflict of interest: The authors declare no competing financial interests.

Acknowledgements: The study was funded by NIH grants EY022854 and EY024831 awarded to N.J.G.

Keywords: sensorimotor, superior colliculus, eye movements, threshold, parallel processing, inhibitory gating

Abstract

The motor system prepares for movements well in advance of their execution. In the gaze control system, premotor neurons that produce a burst of activity for the movement are also active leading up to the saccade. The dynamics of preparatory neural activity have been well described by stochastic accumulator models, and variability in the accumulation dynamics has been shown to be correlated with reaction times of the eventual saccade, but it is unclear whether this activity is purely preparatory in nature or has features indicative of a hidden movement command. We explicitly tested whether preparatory neural activity in premotor neurons of the primate superior colliculus has "motor potential". We removed inhibition on the saccadic system using reflex blinks, which turn off downstream gating, and found that saccades can be initiated before underlying activity reaches levels seen under normal conditions. Accumulating low-frequency activity was predictive of eye movement dynamics tens of milliseconds in advance of the actual saccade, indicating the presence of a latent movement command. We also show that reaching threshold is *not* a necessary condition for movement initiation, contrary to the postulates of accumulation-to-threshold models. The results bring into question extant models of saccade generation and support the possibility of a concurrent representation for movement preparation and generation.

Significance Statement

How the brain plans for upcoming actions before deciding to initiate them is a central question in neuroscience. Popular theories suggest that movement planning and execution occur in serial stages, separated by a decision boundary in neural activity space (e.g., "threshold"), which needs to be crossed before the movement is executed. By removing inhibitory gating on the motor system, we show here that the activity required to initiate a saccade can be flexibly modulated. We also show that evolving activity related to movement planning is a hidden motor command. The results have important implications for our understanding of how movements are generated, in addition to providing useful information for decoding movement intention based on planning-related activity.

Impact Statement

Non-invasive disinhibition of the oculomotor system shows that ongoing preparatory activity in the superior colliculus has movement-generating potential, and need not rise to threshold in order to produce a saccade.

Introduction

The ability to interact with the world through movements is a hallmark of the animal kingdom. Movements are usually preceded by a period of planning, when the nervous system makes decisions about the optimal response to a stimulus and programs its execution. Such planning behavior is seen in a wide variety of species, including, insects (Fotowat and Gabbiani, 2007; Card and Dickinson, 2008), fish (Preuss et al., 2006), frogs (Nakagawa and Nishida, 2012), and mammals (Hanes and Schall, 1996; Churchland et al., 2006a). A fundamental question in sensorimotor neuroscience is how the brain prepares for movements before issuing the command to initiate them.

In the primate gaze control system, premotor neurons that produce a volley of spikes to generate a movement are typically also active leading up to the movement. Build-up of low frequency activity prior to the saccade command, or its signatures, have been observed in a wide variety of brain regions involved in gaze control, including the frontal eye fields (Hanes and Schall, 1996; Gold and Shadlen, 2000), lateral intraparietal area (Platt and Glimcher, 1999), and superior colliculus (SC) (Dorris et al., 1997). Since variability in the onset and rate of accumulation of low-frequency activity is correlated with eventual saccade reaction times (Hanes and Schall, 1996; Ratcliff and Rouder, 1998; Usher and McClelland, 2001), it is thought that this activity primarily dictates *when* the movement is supposed to be initiated. However, it is unclear how downstream motor networks distinguish activity related to movement planning from the command to execute one.

One possibility is that the activity of premotor neurons undergoes a transformation from representing preparation into movement-related commands at a discrete point in time (Thompson et al., 1996; Horwitz and Newsome, 1999; Juan et al., 2004; Schall et al., 2011), when the activity reaches a movement initiation criterion, thereby acquiring the potential to generate a movement. Indeed, this is the basis for stochastic accumulator models of saccade initiation, in which premotor activity must reach a threshold level in order to generate the movement (Hanes and Schall, 1996; Ratcliff and Rouder, 1998; Zandbelt et al., 2014). Recent work in the skeletomotor system has also suggested that neuronal population activity

undergoes a state space transformation just prior to the movement, thus permitting movement preparation without execution (Churchland et al., 2012; Kaufman et al., 2014). These related views dictate that movement planning and execution are implemented as serial processes in the motor system. Alternatively, it is possible that neurons in sensorimotor structures represent these signals concurrently, gearing up to execute a movement in proportion to the strength of the planning activity. Under such parallel implementation, preparatory build-up of neural activity can multiplex higher order signals while simultaneously relaying those signals to effectors. This idea is in fact the premise of the premotor theory of attention (Rizzolatti et al., 1987; Hoffman and Subramaniam, 1995).

How might we test for the presence of such a "motor potential" in low frequency preparatory activity? The following thought experiment helps illustrate one approach. Consider the activity of a premotor neuron accumulating over time. Under normal circumstances, inhibitory gating on the saccadic system is released at an internally specified time, possibly when activity crosses a purported threshold level or when the population dynamics reaches the optimal subspace, generating a movement (top row in Figure 1a). We can then infer that the high frequency movement burst has motor potential if neural activity is correlated with dynamics of the ensuing movement, i.e., saccade velocity is faster when burst activity is higher, and vice versa (match gray traces between top and bottom rows in Figure 1a). Now, if inhibition was somehow removed at a prior time through an experimental manipulation instead of allowing the system its natural time course (thick red line in Figure 1b), the occurrence of a movement would indicate that ongoing neural activity also possesses motor potential. Importantly, this potential can be quantified by correlating neural activity with kinematics of the eye *before* the onset of the saccade and comparing it to the previously estimated potential after saccade onset (velocity traces before saccade onset in Figure 1b). Furthermore, the dynamics of activity following the manipulation would indicate whether the activity must cross a decision boundary in order to produce the movement (dashed traces in Figure 1b). This hypothetical manipulation would therefore simultaneously shed light on both the question of concurrent processing of preparatory signals and the criterion for movement initiation.

In this study, we used the trigeminal blink reflex to remove inhibition on the gaze control network during ongoing low-frequency activity. The omnipause neurons (OPNs) in the brainstem, which discharge at a tonic rate during fixation and are suppressed during saccades (Figure 1c, Cohen and Henn, 1972; Keller, 1974), also become quiescent during eye movements associated with blinks (Schultz et al., 2010). Previous work in our lab has shown that removal of this potent source of inhibition on the saccade burst generators with reflex blinks triggers saccades at lower-than-normal latencies (Gandhi and Bonadonna, 2005), an observation that has been used to study latent sensorimotor processing in SC (Jagadisan and Gandhi, 2016), the motor potential of a target selection signal during visual search (Katnani and Gandhi, 2013), and the dynamics of movement cancellation during saccade countermanding (Walton and Gandhi, 2006). Here, we first established that the saccade-related burst in SC has motor potential under normal conditions, by correlating the activity during the burst to saccade kinematics on individual trials. Critically, in the perturbation condition, we found that the level of preparatory activity at the time of the blink was also strongly correlated with initial dynamics of the evoked movement, *prior* to the saccade proper, suggesting that ongoing sub-threshold activity in SC also possesses motor potential. Finally, we show that although these movements were preceded by an acceleration of ongoing activity following the perturbation, it is not necessary for preparatory activity in SC to reach a threshold before a saccade is produced – neural activity just prior to saccades triggered by reflex blinks was lower at both individual neuron and population levels.

Results

In order to explicitly test whether saccade preparatory activity contains a latent movement command, we induced reflex blinks during the preparatory period in monkeys performing the delayed saccade task (see Methods – visual stimuli and behavior). We first describe important aspects of the blink technique here. A reflex blink is a suitable perturbation because it removes inhibition on the saccadic system by turning off the OPNs and triggers gaze shifts at lower-than-normal latencies (Gandhi and Bonadonna, 2005). We

computed onset times of saccades embedded in blink-triggered movements using an approach that exploited the occurrence of a blink-related eye movement (BREM). Briefly, saccade onset was determined as the time at which the movement velocity on a given trial deviated from the expected BREM profile distribution for that session. Figure 2a shows illustrative examples from one session (left column - temporal velocity profiles, right column - spatial eye position traces). As seen from the three example trials (colored traces in Figure 2a), there was considerable variation in the time at which the eye movement deviated from the BREM profile (thick black traces in Figure 2a; only the mean BREM trace is shown in the right panel for clarity) towards the saccade goal, marking saccade onset. Figure 2b shows the distribution of saccade onset times relative to perturbation time obtained using this approach (for more details, see Methods – movement detection). It is worth noting here that the bimodality apparent in the distribution of saccade onset times in Figure 2b likely reflects the divide between trials in which the process behind saccade initiation was already underway by the time of the blink (delays <20 ms, to the left of the vertical black line), and trials in which the saccade was triggered *due* to disinhibition by the blink (delays >20 ms, to the right of the vertical black line). Since most analyses in this study were focused on processes occurring before saccade onset, we split the data from perturbation trials into two sets, along the aforementioned divide: blink-triggered movements with saccade onset greater than 20 ms were used for accumulation rate and motor potential analyses, and all blink-triggered movements were used for the threshold analysis (for more details, see Methods – inclusion criteria).

The blink perturbation triggers reduced latency, but accurate, saccades

First, we verified that this combination of reflex blinks and saccade detection approach produced low-latency saccades. Figure 3a shows saccade reaction time (from GO cue) as a function of the time of blink in perturbation trials (red circles). To visually compare reaction times on blink trials with those in control trials, it was necessary to include the distribution of control reaction times in this figure. To do this, we created a surrogate dataset by randomly assigning blink times to control trials (see Methods – surrogate

data and statistics), and plotted them on the same axes as blink trials in Figure 3a (blue circles). Reaction times in perturbation trials were correlated with time of blink, and were significantly lower than control reaction times (mean control reaction time = 277 ms, mean blink-triggered reaction time = 227 ms, $p < 10^{-10}$, one-tailed t-test), consistent with previous observations (Gandhi and Bonadonna, 2005).

We then verified whether saccades triggered by the blink were as accurate as normal saccades, in order to eliminate any potential confounds due to differences in accuracy. We calculated saccade accuracy as the Euclidean endpoint error normalized with respect to target location (inset in Figure 3b). The distribution of relative errors for all control and blink trials is shown in Figure 3b. Blink-triggered saccade accuracy was not significantly different from control saccades (mean control accuracy = 0.135, mean blink-triggered accuracy = 0.133, $p = 0.3$, two-tailed t-test). The blink perturbation thus provides an assay to study the question of motor potential without introducing confounding factors related to saccade metrics.

SC activity is correlated with saccade kinematics for normal saccades

Next, as a crucial prerequisite for our motor potential analysis, we verified whether the motor burst in SC is correlated with saccade kinematics. Though it is well-known that the locus activity on the SC map determines amplitude and direction of the saccade vector (see Gandhi and Katnani, 2011, for a review), it is unknown, to the best of our knowledge, whether the instantaneous firing rate of SC neurons drives saccade kinematics, e.g., instantaneous velocity. Therefore, to determine whether a relationship exists between SC activity and saccade velocity, we computed the correlation between the trial-by-trial firing rates of a neuron and the corresponding velocities. This approach to estimating motor potential is illustrated in Figure 4a. Since our eventual goal was to study pre-saccade motor potential in blink-triggered saccades, we used the component of velocity in the direction of the saccade goal as our kinematic variable on a given trial, for the sake of uniformity (inset in Figure 4a, see next section for clarification, and Methods – kinematic variables, for details). We also performed the analysis on the raw,

unprojected kinematics and obtained very similar results (Supplementary Figure 1). Further, to avoid assumptions about the efferent delay between SC activity and ocular kinematics, we computed the activity-velocity correlation at various potential delays between the two signals (the blue bars in Figure 4a show an example delay of 12 ms – compare the similarly shaded bars in the velocity and activity panels). Figure 4b shows, for an example neuron, the trial-by-trial scatter of velocities at three time points (15 ms before, at, and 15 ms after saccade onset – light, medium, and dark blue circles, respectively) plotted against neural activity preceding those respective velocities by 12 ms.

It is not surprising to see a lack of correlation with SC activity for pre-saccade velocities, since they are largely zero or constant, by definition, for normal saccades, and the inhibitory gating by OPNs has not been removed yet. However, the strong correlation between kinematics and activity following movement onset indicates the presence of a motor potential in the saccade-related burst. We systematically explored the time course of this motor potential by computing the correlation at different time points before and during the saccade, for a range of delays between activity and kinematics. We did this for each neuron, and the population average correlation coefficients at each time point and delay are shown in the heat map in Figure 4c. To aid interpretation of this figure, the light blue asterisk in the heat map refers to the correlation computed at the time points with the corresponding asterisk in Figure 4a. Motor potential of SC activity emerged only after the onset of the saccade, and lasted throughout the movement (streak of correlation below the unity line in Figure 4c).

For each time point in the velocity signal, we also computed the activity time points at which correlation was highest, shown as the running mean (black trace) in the heat map. This provides a measure of the efferent delay at which neural activity is most effective in driving movement kinematics. Note that the black trace is roughly parallel to the unity line, suggesting that the efferent delay was consistent for the duration of the movement. To characterize this property better, we plotted optimal efferent delay, calculated as the difference between the black trace and the unity line, as a function time with respect to movement onset (Figure 4d). The mean delay during the movement was -12 ms, meaning that

instantaneous saccade kinematics were best predicted by SC activity 12 ms before. The values for the delay before saccade onset are likely due to noise in the pre-saccade velocities and should be ignored (moreover, note that these delays are positive and therefore non-causal). Finally, Figure 4e shows the correlation values at the -12 ms delay as a function of time. The gray region is the +/- 95% confidence intervals of the population average bootstrapped (trial-shuffled) distribution of correlations. Thus, for normal trials, motor potential, in the form of correlation between neural activity and eye velocity, only manifests after the onset of the saccade proper ($p<0.05$ starting 3 ms after saccade onset).

SC preparatory activity preceding the saccade-related burst possesses motor potential

Having found a correlation between SC activity and ocular kinematics during saccades, we wanted to know whether the time course of such motor potential could be altered by disinhibiting the saccadic system at an earlier time. Specifically, we wanted to know whether ongoing preparatory activity contained any motor potential before its maturation into a motor command. We hypothesized that, if the low-frequency activity had motor potential, removing inhibitory gating on the system would result in a slow eye movement proportional to the level of activity before accelerating into a saccade. The rationale was that, because the downstream OPNs become quiescent due to the blink (and associated BREM), activity in SC neurons that possessed motor potential would be allowed to drive the burst generators, and subsequently, the eye muscles. In order to test this, we computed the correlation between SC activity and eye velocity before and during blink-triggered saccades in a manner similar to that for control saccades (Figure 5a). Figure 5b shows an example scatter plot of the trial-by-trial activities versus velocities for three time points with respect to saccade onset. It is important to note that we subtracted the BREM component from the blink-triggered saccade velocities before projecting these residuals in the direction of the saccade goal (inset in Figure 5a). This was done to prevent the orthogonal variations in BREM kinematics unrelated to SC activity from masking any underlying motor potential-related correlation,

which we found might be the case when we performed this analysis on the raw velocities for blink-triggered saccades (Supplementary Figures 2a-b).

We then computed the population average correlation at different time points before and after the onset of the high velocity saccade, at different efferent delays, and found that neural activity was highly correlated with saccade kinematics for blink-triggered movements also (correlation after time point 0 in the heat map in Figure 5c). Importantly, activity was also strongly correlated with eye kinematics before saccade onset (time points before 0 in Figure 5c), suggesting that upstream SC activity leaked through to the eye muscles as soon as the OPNs were turned off by the blink, causing activity-related deviations in the kinematics around the BREM. The black trace in Figure 5c also shows that the estimated efferent delay was similar to that observed in control trials and consistent before and after saccade onset. This is better observed in Figure 5d (thick red trace) – the mean delay after saccade onset was -12 ms, equal to the mean delay before saccade onset (up to 30 ms before saccade onset). The time course of efferent delay estimates for control trials from Figure 4d is also overlaid for comparison in Figure 5d (thin blue trace). Figure 5e shows the correlation as a function of time during the blink-triggered movement at these mean pre- and post- saccade optimal delays (thick red trace), with the time course for control trials from Figure 4e overlaid for comparison (thin blue trace). The average correlation across the population was significant (red trace above gray bootstrapped distribution, $p<0.05$) starting 30 ms before onset of the saccadic component and lasting until the end of the movement, reiterating the key result of the study.

Recall that, for control saccades, it made no difference whether the motor potential was computed based on the raw velocity traces or the component of velocity in the direction of the saccade (compare Supplementary Figure 1 and Figure 4), an expected result since instantaneous eye velocity is predominantly in the direction of the saccade goal during control saccades. In contrast, for blink-triggered saccades, the motor potential was revealed only when considering kinematics in the direction of the saccade goal (Figure 5), and not with the unprojected kinematics (Supplementary Figure 2). This observation is important for two reasons. First, it ensures that the pre-saccade motor potential seen during

blink-triggered saccades is not a result of misestimating saccade onset within blink-triggered movements. If the observed pre-saccade correlation resulted solely from estimating saccade onset to be later than the ground truth, i.e., it is actually a peri-saccade correlation in disguise, then it should persist even with the raw, unprojected blink-triggered velocity residuals, and at the same efferent delay as for the peri-saccade correlation. This is because we have already seen that motor potentials exist once the saccade has started. Second, it adds support to the notion of motor potential itself, since the preparatory activity only drives kinematics in the neurons' preferred direction, instead of perturbing movements globally. Note that the time course of motor potential, when it exists, and estimated efferent delay, are remarkably similar across all conditions and analyses (Supplementary Figure 2d-e), including the latent pre-saccade potential seen with the projected kinematics. Put together, these observations strongly suggest pre-saccade preparatory activity indeed possesses motor potential which is revealed when the appropriate correlations between neural activity and kinematic variables are computed.

Blink-triggered saccades are evoked at lower thresholds compared to normal saccades

Next, we used the fact that blink-triggered saccades are evoked at lower latencies to test an influential model of saccade initiation – the threshold hypothesis (Hanes and Schall, 1996). We asked whether it is necessary for activity in SC intermediate layer neurons to reach a fixed activity criterion in order to generate a movement. Previous studies have estimated the threshold for individual neurons by assuming a specific time at which the threshold could be reached before saccade onset or by computing the time, backwards from saccade onset, at which premotor activity starts becoming correlated with reaction time (Hanes and Schall, 1996). Given the heterogeneity of the activity profiles of premotor neurons, we think this approach is too restrictive to obtain an unbiased estimate of the threshold, if any. Instead, we took a non-parametric approach and scanned through possible times at which a putative threshold might be reached prior to saccade onset. Figure 6a shows a snippet of the average normalized population activity aligned on saccade onset for control (blue traces) and blink (red traces) trials. For each neuron in this

population (n = 50), we computed the average activity in 10 ms bins slid in 10 ms increments from 50 ms before to 20 ms after saccade onset (colored windows at the bottom of Figure 6a). If activity on control trials reaches the purported threshold at any one of these times before saccade onset, a comparison with activity in blink trials at that time should reveal the existence, or lack thereof, of a fixed threshold. Figure 6b shows the activity in these bins for control trials plotted against blink trials, colored according to the bins in Figure 6a. Note that the majority of points for early time bins lie below the unity line. Activity on blink trials was significantly lower compared to control activity from 50 ms before to 10 ms after saccade onset (square points, Wilcoxon signed-rank test, $p < 0.0001$). The systematic trend in the linear fits (solid lines) to these points suggests that the activity on blink trials gradually approaches that on control trials; however, the earliest time at which control activity was not different from activity in blink trials was 20 ms after saccade onset (circles) – too late to be considered activity pertaining to a movement initiation threshold. Thus, activity at the population level need not reach a threshold level in order to produce a movement.

Nevertheless, we wanted to know if there exist individual neurons in the population that might obey the threshold hypothesis. For each neuron, we calculated whether activity on blink trials was higher, lower, or not significantly different from activity in control trials, at each time point from -50 before to 20 ms after saccade onset (Wilcoxon rank-sum test, $p<0.001$). The three traces in Figure 6c represent the proportion of neurons that showed each of those three characteristics as a function of time. As late as 10 ms before saccade onset, more than 60% of the neurons had lower activity on blink trials compared to control trials (blue trace), inconsistent with the idea of a fixed threshold. Roughly 30% of the neurons did not exhibit significant differences in activity on blink and control trials at that time point (black trace); however, this observation is insufficient to conclude that the activities in the two conditions were identical, or that it must reach a threshold. Of course, it is possible that some of these neurons belong to a class for which fixed thresholds have been observed in previous studies. Together, these results suggest that it is not

318 necessary for premotor activity in SC intermediate layers to reach a threshold level at the individual
319 neuron or population level in order to produce a movement.

320

321 *Rate of accumulation of SC activity accelerates following disinhibition by the blink*

322 Since SC neurons do not necessarily cross a fixed threshold to produce movements, as we saw above, it is
323 possible that blink-triggered saccades are initiated directly off the ongoing level of preparatory activity.
324 Alternatively, low frequency SC activity may be altered by the blink, even if the saccade is triggered at a
325 lower level compared to control trials. Therefore, we finally studied whether the dynamics of SC activity
326 are modulated by the blink prior to saccade initiation. Since we wanted to test for a change in dynamics
327 before the actual saccade started, we restricted our analysis to the subset of trials in which saccade onset
328 occurred at least 20 ms after blink onset. This restriction reduced our population to 38 neurons. For each
329 neuron, we estimated the rate of accumulation of activity in 20 ms windows before and after blink onset
330 with piecewise linear fits (Figure 7a, dashed red trace and solid lines). It is important to note that while
331 the evolution of premotor activity is commonly modelled as a linear process, the actual dynamics of
332 accumulation may be non-linear, causing spurious changes in linear estimates of accumulation rate over
333 time. To account for this, we created a surrogate dataset of control trials for each neuron, with blink times
334 randomly assigned from the actual distribution of blink times for that session. We then performed linear
335 accumulation fits for the control dataset as well (dashed blue trace and solid lines in Figure 7a). Changes
336 in accumulation rate on control trials following the pseudo-blink should reflect the natural evolution of
337 activity at typical blink times and provide a baseline for comparing any changes observed in blink trials.
338 Figure 7b shows a scatter plot of pre- and post- blink accumulation rates on control and blink trials. Pre-
339 blink rates were not different between the two conditions (light circles, Wilcoxon signed-rank test, $p >$
340 0.5), but post-blink rates were significantly higher on blink trials (dark circles, Wilcoxon signed-rank test,
341 $p < 0.01$). Next, we tested for a change in accumulation rates following the blink by calculating a rate
342 change index, defined as the difference of post- versus pre- blink rates divided by their sum, for each

condition (Figure 7c). This index was positive for most neurons, even for control trials, highlighting the natural non-linear dynamics mentioned above. The change in accumulation rate was significantly higher following the actual blink on blink trials (Wilcoxon signed-rank test, $p < 0.0001$) compared to after the pseudo-blink on control trials. Thus, removal of inhibition seems to cause an acceleration in the dynamics of ongoing activity in the lead up to a saccade.

Discussion

In this study, we sought to uncover the dynamics of movement preparation and, specifically, test whether a saccade command is embedded in the preparatory activity of SC neurons. We first established a baseline for this question by showing that the saccade-related activity in the intermediate layers of SC has "motor potential" under normal conditions, defined as correlated variability between firing rate and saccade kinematics. Then, by disinhibiting the saccadic system much earlier than its natural time course with a reflex blink, we showed that low-frequency preparatory activity in these neurons also has a latent motor potential, indicating the presence of a hidden movement command. These results suggest that a correlation between neural activity and movement kinematics may only present itself when intermediary gating (in this case presented downstream of SC by the OPNs) between the two observables is turned off. We also found that activity does not necessarily have to reach a threshold at the single neuron or population level in order to initiate the saccade, contrary to the postulates of an influential model of saccade initiation – the threshold hypothesis (Hanes and Schall, 1996).

Mechanisms of movement preparation and execution

Studies on the neural correlates of movement generation have largely focused on the divide between preparatory activity and executive activity, driven mainly by the substantial natural latencies between the cue to perform a movement and its actual execution. Since variability in the properties of post-cue neural

activity is correlated with eventual movement reaction times (Hanes and Schall, 1996; Churchland et al., 2006b), it is thought that this activity is purely preparatory in nature, influencing only *when* the movement is supposed to be initiated, and is devoid of the potential to generate a movement, until just before its execution. Indeed, there is some evidence that movement preparation and execution have distinct neural signatures with a well-defined boundary separating them. Studies of movement preparation in the skeletomotor system have shown that neural activity reaches an optimal subspace before undergoing dynamics that produce a limb movement (Afshar et al., 2011; Churchland et al., 2012). A related idea suggests that activity pertaining to movement preparation evolves in a region of population space that is orthogonal to the optimal subspace, and this dissociation confers neurons the ability to prepare the movement by incorporating perceptual and cognitive information without risking a premature movement (Kaufman et al., 2014). However, in the absence of perturbations to the natural time course of movement generation, or explanatory models linking them to downstream processing, it is unclear whether such neural correlates are the sole causal links to the process of initiating movements.

How do we reconcile these observations with the finding in this study of a latent motor potential in preparatory activity? One possibility is that the oculomotor system operates differently from the skeletomotor system (for more on this, see next section). More generally, it is possible that it is necessary for population activity to be in an optimal, "movement-generating" subspace in order to release inhibition and/or effectively engage downstream pathways leading up to activation of the muscles, but once the motor system has been disinhibited by another means (e.g., the blink perturbation in this study), preparatory activity is read out as if it were a movement command regardless of its population-level features. More studies that causally delink evolving population activity from physiological gating are needed to clarify these mechanisms.

Implications for threshold-based accumulator models

The threshold hypothesis is the leading model of movement preparation and initiation in the gaze control system (Hanes and Schall, 1996). Inspired by stochastic accumulator models of decision-making (Carpenter and Williams, 1995; Ratcliff and Rouder, 1998), this theory posits that saccade initiation is controlled by accumulation to threshold of a motor preparation signal in premotor neurons. However, it is unclear whether the preparatory activity must rise to a fixed biophysical threshold at the level of individual neurons or a population of neurons in order to initiate a saccade (Hanes and Schall, 1996; Zandbelt et al., 2014), or whether there exists a dynamic equivalent to such a threshold (Lo and Wang, 2006). Indeed, it has recently been shown that a threshold computed under the static assumption can vary across task conditions or epochs, thus challenging the classic interpretation of the threshold hypothesis (Jantz et al., 2013).

Other recent studies have argued that the fixed threshold hypothesis does not hold true for most neurons in SC and FEF (Jantz et al., 2013), finding that the effective threshold varies based on the task being performed by the subject. However, comparison of thresholds across tasks is subject to the confound that the network may be in a different overall state, thereby modulating the threshold. For instance, the presence or absence of the fixation spot at the time of movement initiation, or the presence of other visual stimuli or distractors, may affect how downstream neurons receiving premotor activity from the whole network decode the level of activity, thus influencing the effective threshold. In our study, thresholds are compared between interleaved perturbation and control trials in the *same* behavioral paradigm, eliminating the effect of network-level confounds.

Note that the effective reduction in threshold (or equivalently, non-existence of threshold) that we observe is likely due to reduced activity of the OPNs, which are a potent source of inhibition on the pathway downstream of the SC - premotor activity has to overcome lower inhibition and therefore triggers movements from a lower level. It is also important to note that while there is some evidence that premotor activity in SC is attenuated when saccades are perturbed by a reflex blink (Goossens and Van Opstal, 2000b), we did not observe suppression during movements that were triggered by the blink, as seen in the

firing rate profile in Figure 7a. Nevertheless, the presence of any attenuation would only strengthen the result, since the occurrence of saccades despite attenuated SC activity goes against the notion of a rigid threshold. It has also been suggested that the threshold may not be rigid at the single neuron level but may instead be implemented by pooling the activity of the premotor neuron population (Zandbelt et al., 2014). However, population-level thresholding does not seem like a necessary condition either, based on the results observed in this study (Figure 6a).

Parallel implementation of the sensory-to-motor transformation

An influential idea in systems neuroscience is the premotor theory of attention, which posits that spatial attention is manifested by the same neural circuitry that produces movements (Rizzolatti et al., 1987). Consistent with this hypothesis, studies with cleverly designed behavioral tasks have attributed low-frequency build-up of activity in premotor neurons to a number of cognitive processes, including target selection (Schall and Hanes, 1993; Horwitz and Newsome, 1999; McPeek and Keller, 2002; Carello and Krauzlis, 2004), attention (Goldberg and Wurtz, 1972; Ignashchenkova et al., 2004; Thompson et al., 2005), decision-making (Newsome et al., 1989; Gold and Shadlen, 2000), working memory (Sommer and Wurtz, 2001; Balan and Ferrera, 2003), and reward prediction (Platt and Glimcher, 1999; Hikosaka et al., 2006). However, such multiplexing of cognitive signals along with movement preparation and execution-related activity by premotor neurons only provides circumstantial evidence in support of the premotor theory, leaving open the question of whether the low-frequency activity exclusively represents cognitive and preparatory processes, devoid of a concurrent potential to generate a movement.

Efforts to delineate spatial attention and movement intention by means of causal manipulations have produced a mixed bag of results, with some studies supporting disjoint processing (Juan et al., 2004) and others supporting concurrent processing (Moore and Armstrong, 2003; Katnani and Gandhi, 2013). The strongest piece of evidence yet for concurrent processing is the observation that many of these premotor

neurons also discharge following the onset of a visual stimulus (Wurtz et al., 2001), which can make its way down to effectors resulting in an electromyographic response, e.g., in the neck (Corneil et al., 2004). The discovery of a latent motor potential in the preparatory activity of SC neurons significantly advances this debate by suggesting that while the low-frequency build-up may not trigger movements under normal conditions, movement intention and motor programming signals are also encoded by these neurons in parallel. Moreover, unlike manipulations such as microstimulation or pharmacological inactivation that introduce extrinsic signals that may corrupt the natural processing of this activity, reflex blinks are non-invasive and are likely to provide a more veridical readout of ongoing processes.

It is worthwhile to end on a note of caution. The results in this study are based on experiments performed in one node, SC, in a distributed network of brain regions involved in gaze control. Traditional knowledge imposes a hierarchy on the sensorimotor transformations that need to occur before a gaze shift is generated (Wurtz et al., 2001). It is possible that sensorimotor neurons in SC, and to some extent, FEF, which project directly to the brainstem burst generators (Segraves, 1992; Rodgers et al., 2006), are more likely to exhibit signatures of a motor potential in preparatory activity compared to regions higher in the cascade. Neurons in other regions may still need to signal the initiation of a movement by reaching a threshold, optimal subspace, or other similar decision bound. Furthermore, it is known that movement initiation thresholds in SC and FEF can vary based on task context (e.g., Jantz et al., 2013). The results presented here are based on a relatively simple task – the delayed saccade task. The mechanisms of movement initiation, and the presence of motor potential in preparatory activity, could in principle be different in more complex tasks, e.g. those that involve competitive spatial selection of movements or sequential movements. Future studies that take causal approaches to perturbing intrinsic population dynamics in various premotor areas across different tasks and effector modalities are essential in order to gauge whether the findings in this study point to a fundamental and generalizable property of sensorimotor systems.

Methods

General and surgical procedures

All experimental and surgical procedures were approved by the Institutional Animal Care and Use Committee at the University of Pittsburgh and were in compliance with the US Public Health Service policy on the humane care and use of laboratory animals. We used two adult rhesus monkeys (*Macaca mulatta*, 1 male and 1 female, ages 8 and 10, respectively) for our experiments. Under isoflurane anesthesia, a craniotomy that allowed access to the SC was performed and a recording chamber was secured to the skull over the craniotomy. In addition, posts for head restraint and scleral search coils to track gaze shifts were implanted. Post-recovery, the animal was trained to perform standard eye movement tasks for a liquid reward.

Visual stimuli and behavior

Visual stimuli were displayed by back-projection onto a hemispherical dome. Stimuli were white squares on a dark grey background, 4x4 pixels in size and subtended approximately 0.5° of visual angle. Eye position was recorded using the scleral search coil technique, sampled at 1 kHz. Stimulus presentation and the animal's behavior were under real-time control with a LabVIEW-based controller interface (Bryant and Gandhi, 2005). After initial training and acclimatization, the monkeys were trained to perform a delayed saccade task. The subject was required to initiate the trial by looking at a central fixation target. Next, a target appeared in the periphery but the fixation point remained illuminated for a variable 500-1200 ms, and the animal was required to delay saccade onset until the fixation point was extinguished (GO cue). Trials in which fixation was broken before peripheral target onset were removed from further analyses. The animals performed the task correctly on >95% of the trials.

Induction of reflex blinks

On 15-20% of trials, fixation was perturbed by delivering an air puff to the animal's eye to invoke the trigeminal blink reflex. Compressed air was fed through a pressure valve and air flow was monitored with a flow meter. To record blinks, we taped a small Teflon-coated stainless steel coil (similar to the ones used for eye tracking, but smaller in coil diameter) to the top of the eyelid. The air pressure was titrated during each session to evoke a single blink. Trials in which the animal blinked excessively or did not blink were excluded from further analyses. The air-puff delivery was randomly timed to evoke a blink either during fixation (400-100 ms before target onset) or 100-250 ms after the GO cue, during the early phase of the typical saccade reaction time. The blink evoked during fixation produced a slow and loopy blink-related eye movement (BREM). The eyes returned to near the original position and fixation was re-established for 400-100 ms before a target was presented in the periphery and the remainder of the delayed saccade task continued. The window constraints for gaze were relaxed for a period of 200-500 ms following delivery of the air puff to ensure that the excursion of the BREM did not lead to an aborted trial. The blink evoked after the GO cue typically produced a blink-triggered movement that can be described as a combination of a BREM and a saccade to the desired target location. We used deviations from the BREM profile to determine true saccade onset, as described in more detail in the next section. We also verified whether the endpoint accuracy of blink-triggered movements was similar to that of normal saccades, in order to ensure that accuracy was not a potential confound in the analyses. Blink-triggered movements were as accurate as normal saccades (see Figure 3b), consistent with previous reports (Goossens and Van Opstal, 2000a).

Movement detection

Data were analyzed using a combination of in-house software and Matlab. Eye position signals were smoothed with a phase-neutral filter and differentiated to obtain velocity traces. Normal saccades,

BREMs, and blink-triggered gaze shifts were detected using standard onset and offset velocity criteria (50 deg/s and 30 deg/s, respectively). Onsets and offsets were detected separately for horizontal and vertical components of the movements and the minimum (maximum) of the two values was taken to be the actual onset (offset). Saccade onset times within blink-triggered movements were detected using a non-parametric approach. We first created an estimate of the expected BREM distribution during each session by computing the instantaneous mean and standard deviation of the horizontal and vertical BREM velocity profiles. Then, for each blink-triggered movement in that session, we determined the time point at which the velocity exceeded the +/- 2.5 s.d. bounds of the BREM profile distribution, and remained outside those bounds for at least 15 successive time points. We did this separately for the horizontal and vertical velocity profiles, and took the earlier time point between the two components as the onset of the saccade. We further manually verified that the detected saccadic deviations on individual trials were reasonable, esp., in the spatial domain. Figure 2a illustrates this approach for three example trials.

Electrophysiology

During each recording session, a tungsten microelectrode was lowered into the SC chamber using a hydraulic microdrive. Neural activity was amplified and band-pass filtered between 200 Hz and 5 kHz and fed to a digital oscilloscope for visualization and spike discrimination. A window discriminator was used to threshold and trigger spikes online, and the corresponding spike times were recorded. The location of the electrode in the SC was confirmed by the presence of visual and movement-related activity as well as the ability to evoke fixed vector saccadic eye movements at low stimulation currents (20-40 μA, 400 Hz, 100 ms). Before beginning data collection for a given neuron, its response field was roughly estimated. During data collection, the saccade target was placed either in the neuron's response field or at the diametrically opposite location (reflected across both axes) in a randomly interleaved manner.

Data analysis – neural pre-processing

Raw spike density waveforms were computed for each neuron and each trial by convolving the spike trains with a Gaussian kernel. We used a 4 ms wide kernel for analyses that involved trial-averaged neural activity and a 10 ms kernel for analyses that were performed on individual trial activity. For a given neuron and target location, spike densities were averaged across trials after aligning to target and saccade onsets. Neurons were classified as visual, visuomovement or movement-related, based on the presence of a significant target and/or saccade-related response. We only analyzed visuomovement and movement neurons for this study, the majority of which were visuomovement (47/50). Where necessary, we normalized the trial-averaged spike density of each neuron to enable meaningful averaging across the population. The activity of each neuron was normalized by its peak trial-averaged firing rate during normal saccades.

Data analysis – inclusion criteria

For all analyses, we only considered neurons for which we had at least 10 blink perturbation trials. Since we only introduced the blink perturbation on a small percentage of trials in a given session in order to prevent habituation, this restricted our population to 50 neurons. We used all 50 neurons for the threshold analysis (Figure 6). For the motor potential analysis (Figure 5), since our aim was to correlate neural activity with eye kinematics before saccade onset, we used only the subset of trials where the onset of the saccade was delayed with respect to overall movement onset by at least 20 ms. To ensure that the correlation values were reliable, we used only neurons which had at least 10 trials meeting the above criterion. This restriction reduced the number of neurons available for the motor potential analyses to 38, and we used the same neurons for control trials to enable meaningful comparison (Figure 4). For the same reason, we also used this subset of neurons for the accumulation rate analysis (Figure 7), where we

559 compared the dynamics of neural activity in 20 ms windows before and after blink onset, and we wanted
560 to ensure that the post-blink window did not include activity co-occurring with the saccade.

561

562 *Kinematic variables*

563 For the motor potential analyses in Figures 4 and 5, we computed the across-trial correlation between
564 instantaneous movement kinematics and neural activity for each neuron. We computed the kinematic
565 variable of relevance for each analysis as follows. In all cases, we used the raw or modified (see below)
566 horizontal and vertical velocity signals to compute a single vectorial velocity signal using the Pythagorean
567 theorem: $\boldsymbol{v}(t) = \sqrt{\boldsymbol{v}_h^2(t) + \boldsymbol{v}_v^2(t)}$. For the analyses in Supplementary Figure 1, for control trials, we used
568 the raw, unmodified velocity signals to compute vectorial velocity as a function of time. We used this as
569 the instantaneous kinematic variable to correlate with neural activity. For perturbation trials in
570 Supplementary Figure 2, we first noted that the blink-related eye movement must contribute a substantial
571 velocity component to the overall movement, since the initial phases of velocity and spatial profiles of
572 blink-triggered movements looked largely like those of a BREM (see Figure 2a). Thus, in order to extract
573 only the saccadic component of a blink-triggered movement, we subtracted from it the mean BREM
574 template on a given session, and used only the horizontal and vertical residuals to compute the vectorial
575 residual velocity: $\tilde{v}(t) = \sqrt{\tilde{\boldsymbol{v}}_h^2(t) + \tilde{\boldsymbol{v}}_v^2(t)}$.

576 A potential pitfall when using residual velocities by just subtracting out the mean BREM, given the
577 variability in BREM profiles across repetitions, is that intrinsic variability of the BREM itself may mask
578 any correlated variability that might be present between ocular kinematics and neural activity. In other
579 words, if the BREM is driven by an independent pathway compared to the saccade/SC activity, it
580 represents an orthogonal source of variability in the kinematics relative to the activity-driven variability
581 that is being examined. Therefore, for the perturbation trial analysis in Figure 5, we used the component

of residual velocity in the direction of the saccade goal, to isolate variability in the direction of the saccade. The kinematic variable for this analysis is thus defined as: $\widetilde{v_\theta}(t) = \sqrt{\tilde{\boldsymbol{v}}_h^2(t) + \tilde{\boldsymbol{v}}_v^2(t)}\cos\theta$, where θ is the angle between the instantaneous residual velocity vector and the direction of the saccade goal (e.g., between the green and black vectors in the inset in Figure 5a). For the sake of consistency, we used a similar variable: $\boldsymbol{v_\theta}(t) = \sqrt{\boldsymbol{v}_h^2(t) + \boldsymbol{v}_v^2(t)}\cos\theta$, for the equivalent control analysis in Figure 4, even though the instantaneous direction of velocity is largely towards saccade goal in this condition.

Motor potential estimation

To estimate motor potential, we computed the correlation between instantaneous neural activity and eye kinematics (according to the variables defined above) across trials, at various potential efferent delays between activity and velocity. For each neuron, we computed the Pearson's correlation coefficient $c_{t+\Delta,t} = corr(\boldsymbol{a}(t+\Delta), \boldsymbol{v}(t))$ between the activity vector $\boldsymbol{a}(t) = [a^1(t), \dots, a^n(t)]$ and the kinematics vector $\boldsymbol{v}(t) = [v^1(t), \dots, v^n(t)]$ at time separations or lags $\Delta \in [-50,50]$, where n is the number of trials for that condition for that neuron. Each point in the third panel (panel c) in Figures 4-5 and Supplementary Figures 1-2 thus represents the average correlation coefficient across the population of neurons between firing rate and kinematics at the corresponding time points. Then, to estimate the optimal efferent delay between activity and velocity, we computed the time at which this population average correlation peaks along the activity axis (vertical axis in the panel c heatmaps) for each time point during the movement. A moving average of this efferent delay trace is shown as the black trace in the heatmaps. The vertical distance of this trace from the unity line is equal to the the actual value of the optimal efferent delay at each movement time point, shown in panel d in Figures 4-5 and Supplementary Figures 1-2. We then calculated the mean efferent delay during the movement after saccade onset (and

before saccade onset in the perturbation condition), and plotted the population average correlation at this delay (panel e in the aforementioned figures).

Surrogate data and statistics

For the accumulation rate analysis in Figure 7, we created a surrogate dataset of control trials with blink times randomly sampled from the distribution of blink occurrences in perturbation trials for that session and assigned to individual control trials. For each neuron, we created 1000 such pseudo-trials by resampling from and reassigning to control trials. We then fit the accumulation rates 20 ms before and after the blink with piecewise-linear functions and compared the change in accumulation rates before and after the pseudo-blink in control trials and the blink in perturbation trials. We created a similar surrogate dataset for the purpose of visualization alone for Figure 3a.

To estimate the significance of the correlation profile in the motor potential analyses, we performed a bootstrap analysis on a trial-shuffled dataset using the same procedures laid out in the previous section. For each neuron, we shuffled trial identities between the across-trial activity and velocity vectors, and computed population average correlation as before. The resultant correlation trace at the optimal efferent delay (estimated for the true data) and the 95% confidence interval bounds are shown in panel e in Figures 4-5 and Supplementary Figures 1-2. Correlation values outside these bounds were significant at $p < 0.05$.

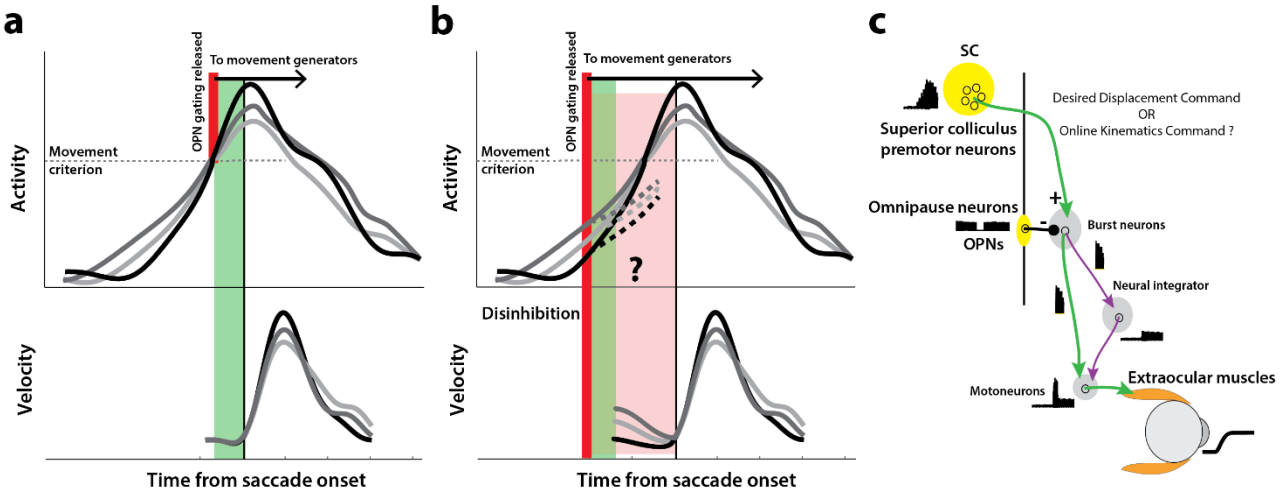

Figure 1. Conceptual schematic of saccade and pre-saccade motor potential revealed by disinhibition. a. Under normal conditions, premotor activity accumulates at different rates on different trials (three example traces in top row) to a movement initiation criterion, opening downstream gating (thick red line) and triggering the saccade following an efferent delay (green window). Following saccade onset, variation in neural activity is correlated with variation in saccade velocity (match gray scale in top and bottom rows), indicating the neuron's motor potential. **b.** Removal of inhibition through an experimental manipulation at an earlier time (thick red line), during saccade preparation and before the typical movement criterion is reached. The disinhibition may reveal the motor potential of ongoing activity in the form of correlated kinematics of the eye before onset of the actual saccade (light red region, velocity traces in bottom row), and also allow us to study any changes in the dynamics of activity leading up to the reduced latency saccades (dashed activity traces in top row). **c.** Schematic of the premotor circuitry involved in saccade generation. A desired displacement command (or, as tested here, a kinematics-driving command) is sent from neurons in SC to the burst neurons in the brainstem reticular formation. This pathway is gated by tonic inhibition from the OPNs under normal conditions. Just prior to saccade initiation, OPN activity pauses, disinhibiting the burst neurons and allowing the excitatory pathway (green arrows) to actuate an eye movement. This study tests whether disinhibiting the pathway downstream of SC by blink-induced suppression of OPNs results in an immediate eye movement.

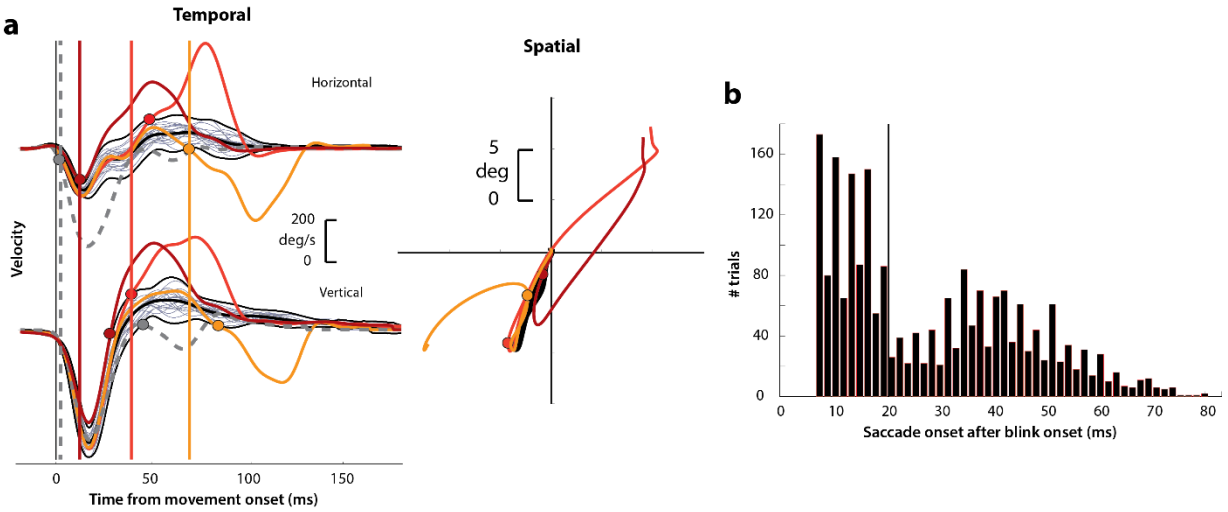

Figure 2. Determining goal-directed saccade onset in blink-triggered eye movements. a. Left column: horizontal (top row) and vertical (bottom row) eye velocity profiles during blink-related eye movements obtained during fixation (BREMs, thin gray traces) and three example blink-triggered saccadic eye movements (colored traces) from one session. The thick black trace in the middle of the BREM profiles is their mean and the two black traces above and below it are +/- 2.5 s.d. bounds. Saccade onset was determined to be the point where an individual velocity profile (colored traces) crossed the BREM bounds and stayed outside for 15 consecutive time points. This point was determined independently for the horizontal and vertical channels (colored circles corresponding to each trace in the two rows), and the earlier time point was taken as the onset of the overall movement (vertical colored lines). The dashed gray velocity profile that deviates from the BREM very close to movement onset (<5 ms) is shown to highlight a case where the saccade starts before being perturbed by the blink, and was not considered as a blink-triggered movement in this study. Right column: Spatial trajectories of the eye for the three example blink-triggered movements from the left column, with the corresponding saccade onset time points indicated by the circles. The trajectory of the BREM template is shown in black (for the sake of clarity, only the mean is shown). Note that the movements in this session were made to one of two possible targets on any given trial. **b.** Distribution of goal-directed saccade onset times relative to movement onset for blink-triggered movements across all sessions. For the motor potential and accumulation rate analyses (Figures 4-5 and 7), we only considered movements where the blink-triggered saccade started at least 20 ms after movement onset (to the right of the vertical line). For the threshold analysis (Figure 6), we considered all blink-triggered movements.

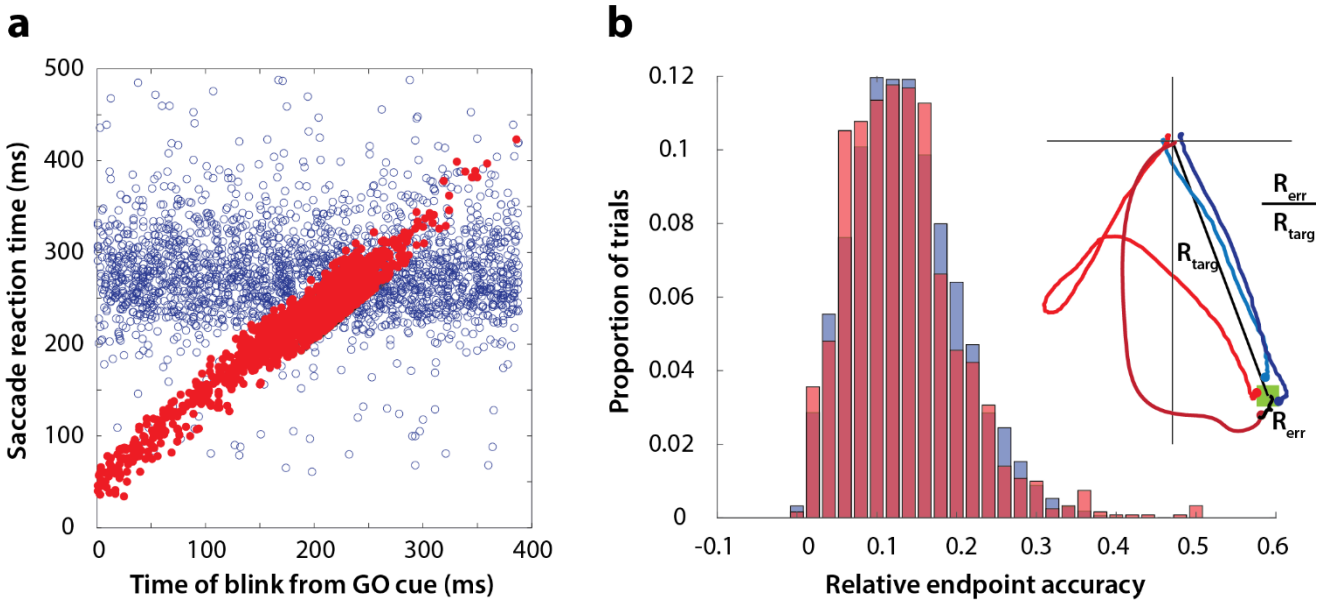

Figure 3. Time course and accuracy of blink-triggered saccades. a. Saccade reaction time as a function of blink onset time. Red filled circles are individual blink trials, and blue circles are from control trials with randomly assigned blink times for comparison. **b.** Endpoint accuracy of control and blink-triggered movements (blue and red histograms) across all trials from all sessions. To enable comparison across movement amplitudes, the endpoint error was normalized as the actual Euclidean endpoint error from the target divided by the eccentricity of the target (inset).

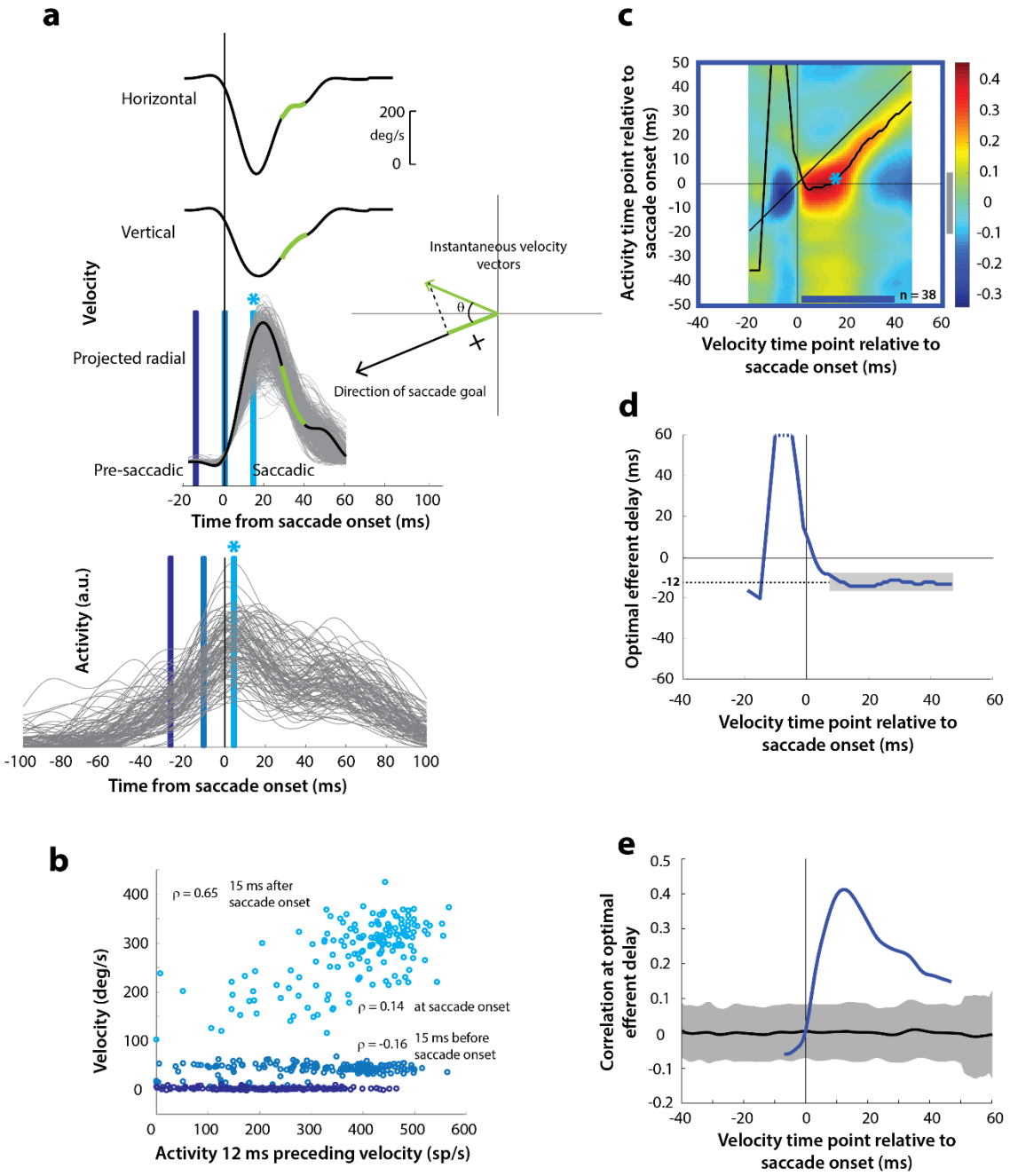

Figure 4. Motor potential during control saccades. a. Estimating motor potential as correlation between neural activity and saccade kinematics. Horizontal and vertical velocity traces (top two rows) on control trials are converted to radial velocity (third row) in the direction of the saccade goal. The projection of the green vector in the inset and the corresponding green parts of the velocity traces illustrate this computation. One trial (thick black trace) is highlighted for clarity. The bottom row shows neural activity traces on different trials for the neuron recorded in this example session. **b.** Motor potential is estimated as the correlation between neural activity and projected saccade kinematics. The scatter plot of the projected radial velocity 15 ms after saccade onset, at saccade onset, and 15 ms before saccade onset (light, medium, and dark blue points, respectively, and corresponding vertical lines in panel a)

against neural activity 12 ms preceding the velocity time points shows that the neuron has motor potential once the saccade has started (Pearson's correlation coefficient = 0.65). Each point corresponds to one trial. **c.** Point-by-point correlation between velocity and activity, averaged across neurons. Heat map colors represent correlation values. As an example, the light blue asterisk refers to the correlation between the velocity and activity corresponding to the time points with the asterisk in panel a. The black curve traces the contour of the highest correlation time points in the activity for each point during the movement. The gray bar next to the color bar represents the average +/- 95% CI for the correlation (see panel e). **d.** Optimal efferent delay computed as the distance of the black trace in panel c from the unity line. Negative values for the delay are causal, i.e., correlation was high for activity points leading the velocity points. The shaded gray bar shows that the optimal delay was consistent during the movement (mean for shaded region = -12 ms) **e.** Population average correlation as a function of time at the -12 ms estimated efferent delay. The black trace is the mean and the gray region is the +/- 95% confidence interval for the bootstrapped (trial-shuffled) correlation distribution.

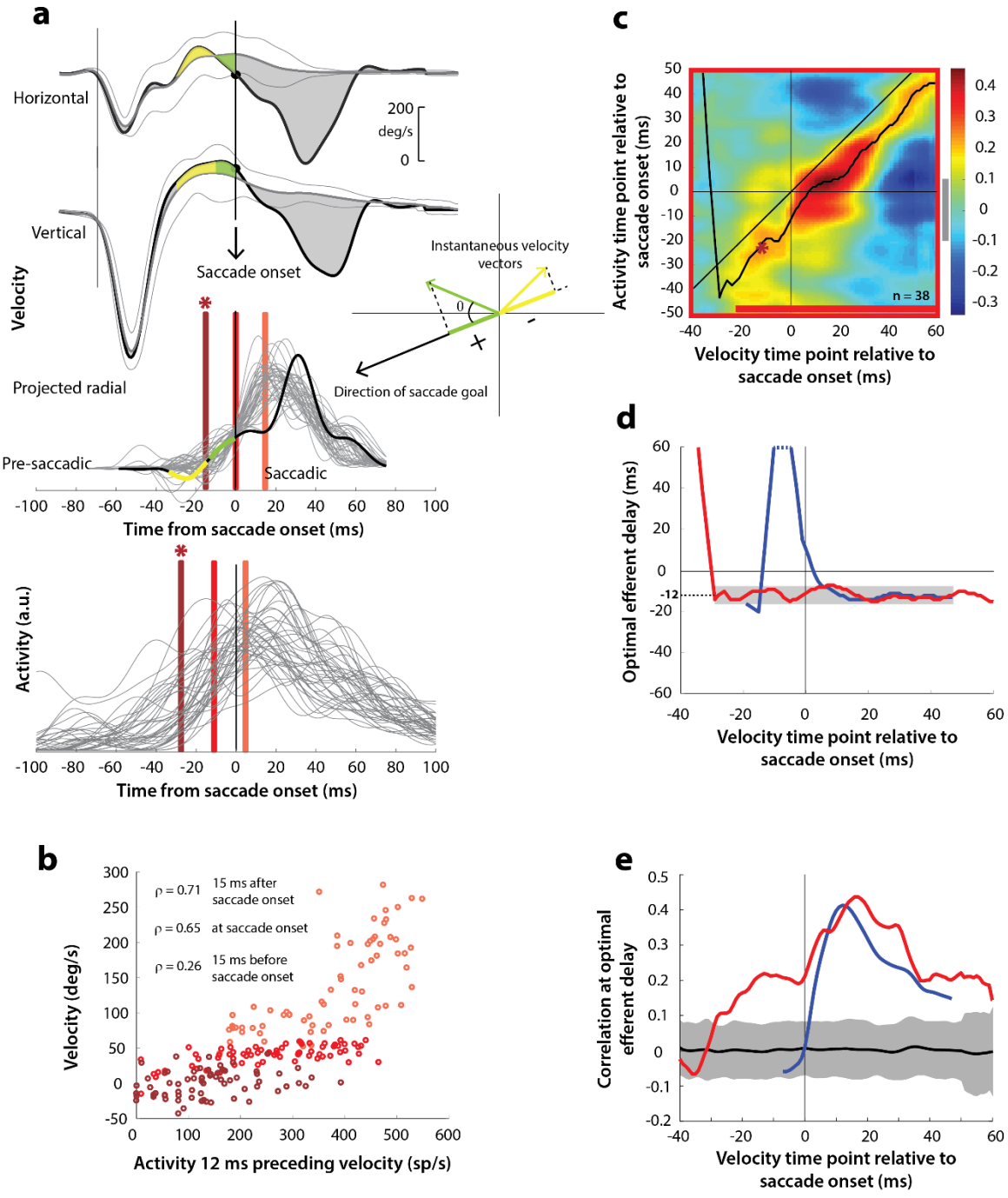

Figure 5. Motor potential on blink trials. a. Computation of the kinematic variable for blink-triggered movements. Horizontal and vertical velocities (thick black traces in top two rows) are converted to residual velocities (gray fill) after subtracting the corresponding mean BREM template (middle thin black trace in top two rows), in order to discount the effects of intrinsic variability in the BREM itself. The radial residual velocity (third row) in the direction of the saccade goal is then computed, similar to Figure 4a. The green and yellow time points in the velocity traces (extended in time for clarity) are represented as corresponding velocity vectors in the inset, illustrate this process. For example, the green velocity residual, immediately before saccade onset, deviates negatively from the BREM in the horizontal

component, and positively in the vertical component, resulting in an instantaneous kinematic vector pointing leftwards and upwards. The component of this vector in the direction of the saccade goal is then taken as the kinematic variable for this time point (also compare Supplementary Figure 2). **b.** Scatter plot of the neural activity versus velocity at the three indicated time points (red points of various saturation, at corresponding red lines in panel a) for blink-triggered movements. As in Figure 4b, these are also plotted at the -12 ms delay between activity and velocity Note the strong correlation for pre-saccade time points compared to Figure 4b. **c.** Point-by-point correlation of velocity and activity, averaged across neurons, for blink-triggered movements. The velocity time points are with respect to time of saccade onset extracted from the blink-triggered movement. The dark red asterisk points to the correlation between the velocity and activity corresponding to the time points with the asterisk in panel a. The black curve traces the contour of the highest correlation time points in the activity for each point during the movement. The gray bar next to the color bar represents the average +/- 95% CI for the correlation (see panel e). **d.** Optimal efferent delay computed as the distance of the black trace in panel c from the unity line. The red trace is for blink-triggered movements, and the blue trace is from Figure 4d for control saccades, overlaid for comparison. Negative values for the delay are causal, i.e., correlation was high for activity points leading the velocity points. The gray bar highlights the fact that the optimal delay was consistent during both control and blink-triggered saccades, and both before and after saccade onset for the latter (mean for shaded region = -12 ms). **e.** Population average correlation for blink-triggered movements (red trace) as a function of time at the -12 ms estimated efferent delay. The blue trace is from Figure 4e for control saccades, overlaid for comparison. The black trace is the mean and the gray region is the +/- 95% confidence interval for the bootstrapped (trial-shuffled) correlation distribution.

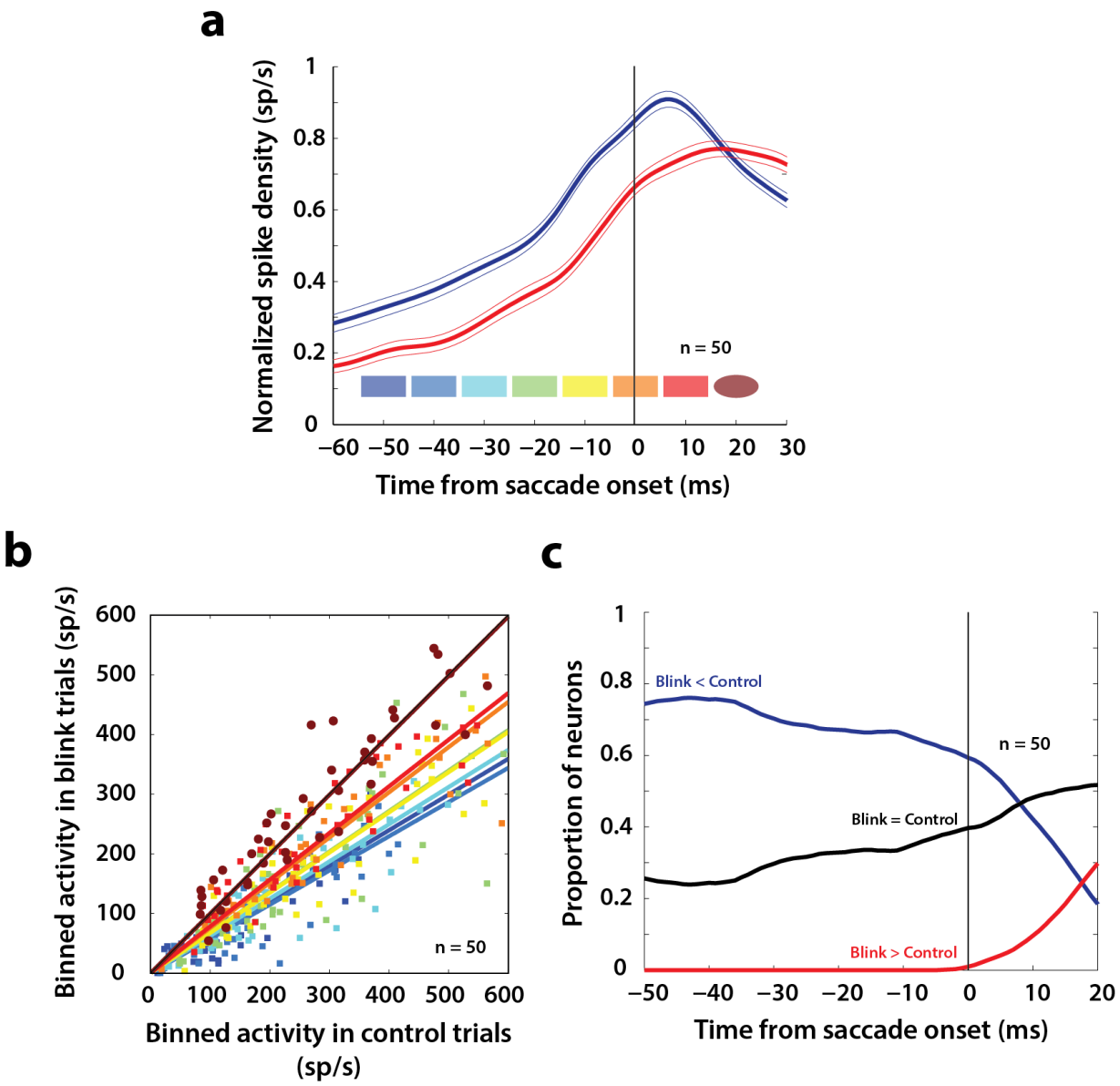

Figure 6. Analysis of putative threshold. a. Average normalized population activity (thick traces) aligned on saccade onset for control (blue trace) and blink (red trace) trials. The thin lines represent s.e.m. The colored swatches at the bottom show the time windows used for the analysis presented in **b**; their shapes represent the presence (rectangle) or absence (ellipse) of a significant difference between control and blink rates in that time window. **b.** Scatter plot of the activities of individual neurons in the time windows illustrated in **a** for control versus blink trials. Square points indicate that the activity in control trials was higher in that window compared to blink trials, and circles indicate that there was no significant difference between the two conditions. Colored lines indicate linear fits to the scatter at the corresponding time window. The diagonal (thin black line) is the unity line; it overlaps with the dark brown line. **c.** Proportion of neurons exhibiting the corresponding labelled differences between the two conditions as a function of time.

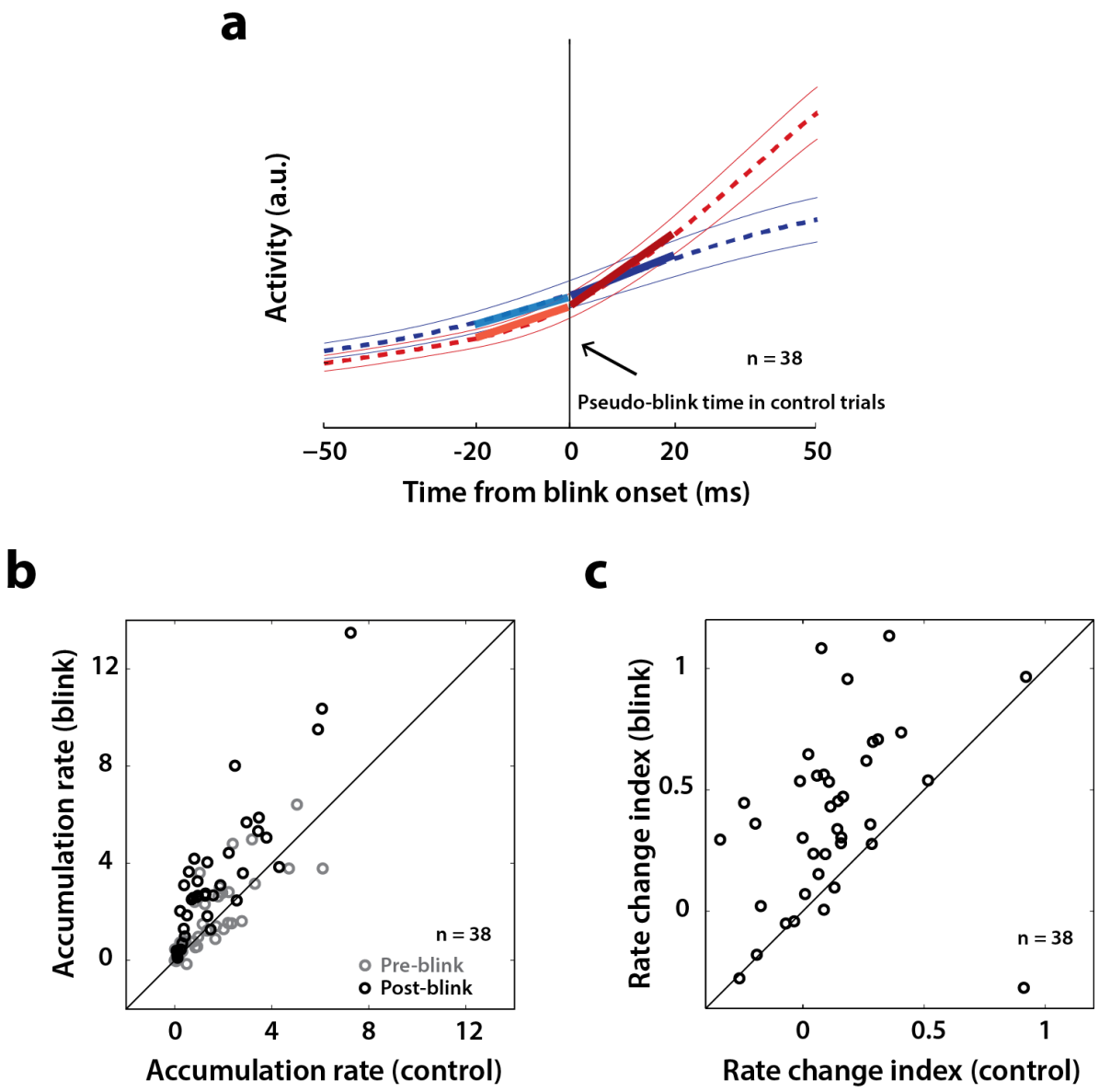

Figure 7. Analysis of accumulation rate change following perturbation. a. Schematic illustrating the computation of accumulation rates before and after the blink. The snippet shows the average population activity centered on blink onset for blink trials (red trace) and pseudo-blink onset from the surrogate dataset for control trials (blue trace). The thick lines represent linear fits to the activity 20 ms before (lighter colors) and after (dark colors) the blink time. **b.** Scatter plot of pre-blink (gray circles) and post-blink (black circles) accumulation rates of individual neurons for control versus blink trials. The unity line is on the diagonal. **c.** Scatter plot of the pre-to-post rate modulation index for control versus blink trials.

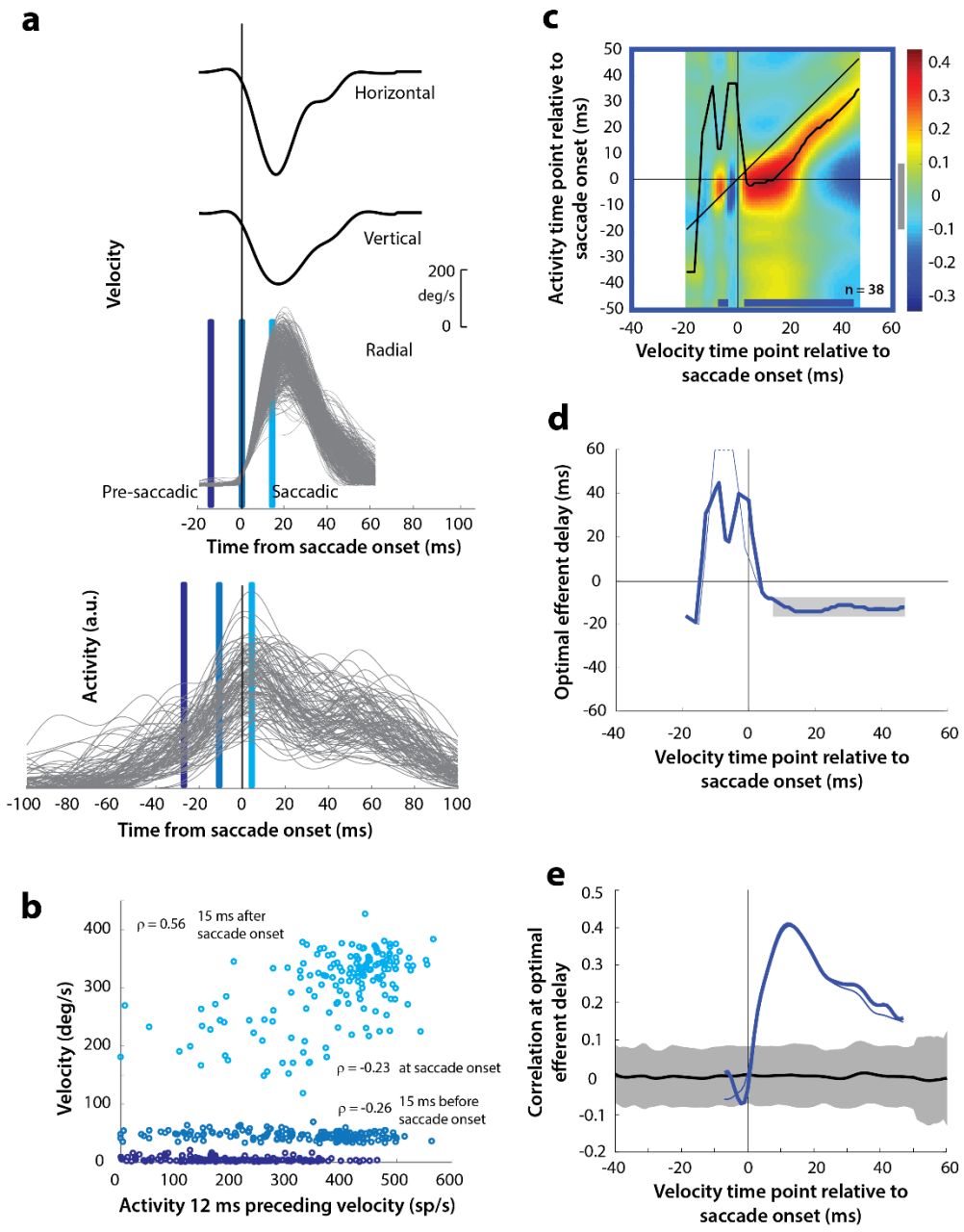

Supplementary Figure 1. Motor potential during control saccades, computed with raw velocities. a. As in Figure 4a, horizontal and vertical velocity traces (top two rows) on control trials are converted to radial velocity (third row). In contrast to Figure 4a, the velocities are used *as is* to compute motor potential, without projecting onto the direction of the saccade goal. The bottom row shows neural activity traces on different trials for the neuron recorded in this example session (same as Figure 4a). **b.** Motor potential is estimated as the correlation between neural activity and saccade kinematics in appropriate time windows. The scatter plot of the projected radial velocity 15 ms after saccade onset, at saccade onset, and 15 ms before saccade onset (light, medium, and dark blue points, respectively, and corresponding vertical lines in panel a) against neural activity 12 ms preceding the velocity time points. Each point corresponds to one trial. **c.** Point-by-point correlation of velocity and activity, averaged across neurons.

The black curve traces the contour of the highest correlation time points in the activity for each point during the movement. The gray bar next to the color bar represents the average +/- 95% CI for the correlation (see panel e). **d.** Optimal efferent delay (thick blue trace) computed as the distance of the black trace in panel c from the unity line. Negative values for the delay are causal, i.e., correlation was high for activity points leading the velocity points. The gray bar shows that the optimal delay was consistent during the movement (-12 ms) **e.** Population average correlation as a function of time at the -12 ms estimated efferent delay. The black trace is the mean and the gray region is the +/- 95% confidence interval for the bootstrapped (trial-shuffled) correlation distribution. The thin traces in panels d-e are from Figures 4d-e, overlaid for comparison.

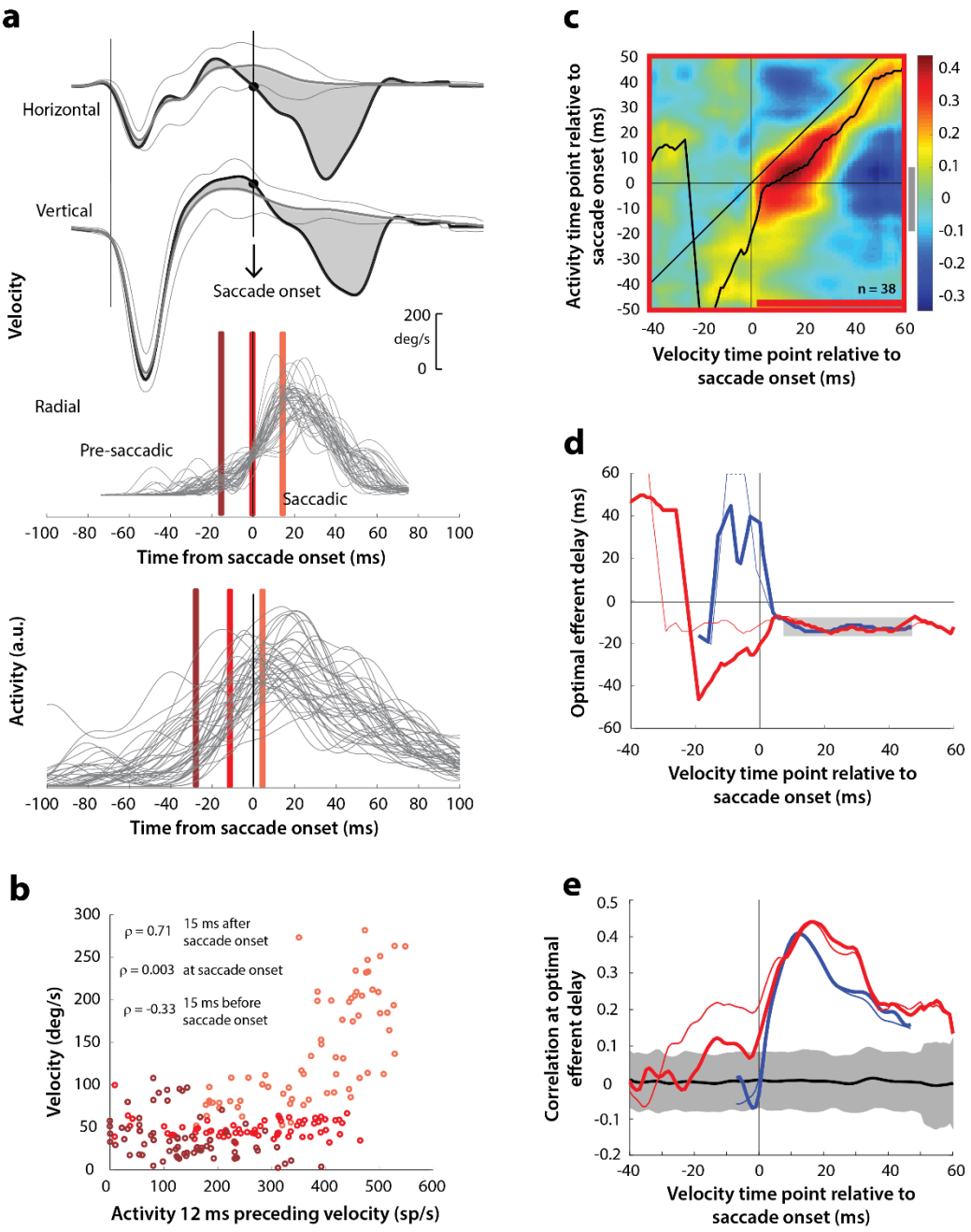

Supplementary Figure 2. Motor potential on blink trials, computed with raw velocities. a. As in Figure 5a, horizontal and vertical velocity traces (top two rows) during blink-triggered movements are converted to radial velocity (third row). In contrast to Figure 5a, the residual velocities (gray shaded deviation from the BREM template) are used *as is* to compute motor potential, without projecting onto the direction of the saccade goal. The bottom row shows neural activity traces on different trials for the neuron recorded in this example session (same as Figure 5a). **b.** Scatter plot of the neural activity versus velocity at the three time points (shaded red windows) from panel a for blink-triggered movements. **c.** Point-by-point correlation of velocity and activity, averaged across neurons, for blink-triggered movements. The velocity time points are with respect to time of saccade onset extracted from the blink-

triggered movement. The black curve traces the contour of the highest correlation time points in the activity for each point during the movement. The gray bar next to the color bar represents the average +/- 95% CI for the correlation (see panel e). **d.** Optimal efferent delay computed as the distance of the black trace in panel c from the unity line. The thick red trace is for blink-triggered movements computing using raw kinematics, and the others are from previous analyses overlaid for comparison (thin red trace is from Figure 5d, thick blue trace is from Supplementary Figure 1d, and thin blue trace is from Figure 4d). Negative values for the delay are causal, i.e., correlation was high for activity points leading the velocity points. The estimated efferent delay after saccade onset was consistent with the result in Figure 5 (mean for shaded region = -12 ms), but note the abrupt deviation from this value in the pre-saccade period, compared to the thin red trace. **e.** Population average correlation for blink-triggered movements (thick red trace) as a function of time at the -12 ms estimated efferent delay. As in panel d, the other traces are from previous analyses, overlaid for comparison. The black trace is the mean and the gray region is the +/- 95% confidence interval for the bootstrapped (trial-shuffled) correlation distribution.

849 **References**

850 Afshar A, Santhanam G, Yu BM, Ryu SI, Sahani M, Shenoy KV (2011) Single-trial neural correlates of
851 arm movement preparation. Neuron 71:555-564.
852 Balan PF, Ferrera VP (2003) Effects of gaze shifts on maintenance of spatial memory in macaque frontal
853 eye field. J Neurosci 23:5446-5454.
854 Bryant CL, Gandhi NJ (2005) Real-time data acquisition and control system for the measurement of
855 motor and neural data. J Neurosci Methods 142:193-200.
856 Card G, Dickinson MH (2008) Visually mediated motor planning in the escape response of Drosophila.
857 Curr Biol 18:1300-1307.
858 Carello CD, Krauzlis RJ (2004) Manipulating intent: evidence for a causal role of the superior colliculus
859 in target selection. Neuron 43:575-583.
860 Carpenter RH, Williams ML (1995) Neural computation of log likelihood in control of saccadic eye
861 movements [see comments]. Nature 377:59-62.
862 Churchland MM, Santhanam G, Shenoy KV (2006a) Preparatory activity in premotor and motor cortex
863 reflects the speed of the upcoming reach. J Neurophysiol 96:3130-3146.
864 Churchland MM, Yu BM, Ryu SI, Santhanam G, Shenoy KV (2006b) Neural variability in premotor
865 cortex provides a signature of motor preparation. J Neurosci 26:3697-3712.
866 Churchland MM, Cunningham JP, Kaufman MT, Foster JD, Nuyujukian P, Ryu SI, Shenoy KV (2012)
867 Neural population dynamics during reaching. Nature 487:51-56.
868 Cohen B, Henn V (1972) Unit activity in the pontine reticular formation associated with eye movements.
869 Brain Res 46:403-410.
870 Corneil BD, Olivier E, Munoz DP (2004) Visual responses on neck muscles reveal selective gating that
871 prevents express saccades. Neuron 42:831-841.
872 Dorris MC, Paré M, Munoz DP (1997) Neuronal activity in monkey superior colliculus related to the
873 initiation of saccadic eye movements. J Neurosci 17:8566-8579.
874 Fotowat H, Gabbiani F (2007) Relationship between the phases of sensory and motor activity during a
875 looming-evoked multistage escape behavior. J Neurosci 27:10047-10059.
876 Gandhi NJ, Bonadonna DK (2005) Temporal interactions of air-puff evoked blinks and saccadic eye
877 movements: Insights into motor preparation. J Neurophysiol 93:1718-1729.
878 Gandhi NJ, Katnani HA (2011) Motor functions of the superior colliculus. Annu Rev Neurosci 34:203-
879 229.
880 Gold JI, Shadlen MN (2000) Representation of a perceptual decision in developing oculomotor
881 commands. Nature 404:390-394.
882 Goldberg ME, Wurtz RH (1972) Activity of superior colliculus in behaving monkey. II. Effect of
883 attention on neuronal responses. J Neurophysiol 35:560-574.
884 Goossens HH, Van Opstal AJ (2000a) Blink-perturbed saccades in monkey. I. Behavioral analysis. J
885 Neurophysiol 83:3411-3429.
886 Goossens HH, Van Opstal AJ (2000b) Blink-perturbed saccades in monkey. II. Superior colliculus
887 activity. J Neurophysiol 83:3430-3452.
888 Hanes DP, Schall JD (1996) Neural control of voluntary movement initiation. Science 274:427-430.
889 Hikosaka O, Nakamura K, Nakahara H (2006) Basal ganglia orient eyes to reward. J Neurophysiol
890 95:567-584.
891 Hoffman JE, Subramaniam B (1995) The role of visual attention in saccadic eye movements. Percept
892 Psychophys 57:787-795.
893 Horwitz GD, Newsome WT (1999) Separate signals for target selection and movement specification in
894 the superior colliculus. Science 284:1158-1161.
895 Ignashchenkova A, Dicke PW, Haarmeier T, Thier P (2004) Neuron-specific contribution of the superior
896 colliculus to overt and covert shifts of attention. Nature neuroscience 7:56-64.

Jagadisan UK, Gandhi NJ (2016) Disruption of fixation reveals latent sensorimotor processes in the superior colliculus. J Neurosci In Press.

Jantz JJ, Watanabe M, Everling S, Munoz DP (2013) Threshold mechanism for saccade initiation in the frontal eye field and superior colliculus. J Neurophysiol 109:2767-2780.

Juan CH, Shorter-Jacobi SM, Schall JD (2004) Dissociation of spatial attention and saccade preparation. Proceedings of the National Academy of Sciences of the United States of America 101:15541-15544.

Katnani HA, Gandhi NJ (2013) Time course of motor preparation during visual search with flexible stimulus-response association. J Neurosci 33:10057-10065.

Kaufman MT, Churchland MM, Ryu SI, Shenoy KV (2014) Cortical activity in the null space: permitting preparation without movement. Nature neuroscience 17:440-448.

Keller EL (1974) Participation of medial pontine reticular formation in eye movement generation in monkey. J Neurophysiol 37:316-332.

Lo CC, Wang XJ (2006) Cortico-basal ganglia circuit mechanism for a decision threshold in reaction time tasks. Nature neuroscience 9:956-963.

McPeek RM, Keller EL (2002) Saccade target selection in the superior colliculus during a visual search task. J Neurophysiol 88:2019-2034.

Moore T, Armstrong KM (2003) Selective gating of visual signals by microstimulation of frontal cortex. Nature 421:370-373.

Nakagawa H, Nishida Y (2012) Motor planning modulates sensory-motor control of collision avoidance behavior in the bullfrog, Rana catesbeiana. Biol Open 1:1094-1101.

Newsome WT, Britten KH, Movshon JA (1989) Neuronal correlates of a perceptual decision. Nature 341:52-54.

Platt ML, Glimcher PW (1999) Neural correlates of decision variables in parietal cortex. Nature 400:233-238.

Preuss T, Osei-Bonsu PE, Weiss SA, Wang C, Faber DS (2006) Neural representation of object approach in a decision-making motor circuit. J Neurosci 26:3454-3464.

Ratcliff R, Rouder JN (1998) Modeling response times for two-choice decisions. Psychol Rev 9:347-356.

Rizzolatti G, Riggio L, Dascola I, Umilta C (1987) Reorienting attention across the horizontal and vertical meridians: evidence in favor of a premotor theory of attention. Neuropsychologia 25:31-40.

Rodgers CK, Munoz DP, Scott SH, Pare M (2006) Discharge properties of monkey tectoreticular neurons. J Neurophysiol 95:3502-3511.

Schall JD, Hanes DP (1993) Neural basis of saccade target selection in frontal eye field during visual search. Nature 366:467-469.

Schall JD, Purcell BA, Heitz RP, Logan GD, Palmeri TJ (2011) Neural mechanisms of saccade target selection: gated accumulator model of the visual-motor cascade. Eur J Neurosci 33:1991-2002.

Schultz KP, Williams CR, Busettini C (2010) Macaque pontine omnipause neurons play no direct role in the generation of eye blinks. J Neurophysiol 103:2255-2274.

Segraves MA (1992) Activity of monkey frontal eye field neurons projecting to oculomotor regions of the pons. J Neurophysiol 68:1967-1985.

Sommer MA, Wurtz RH (2001) Frontal eye field sends delay activity related to movement, memory, and vision to the superior colliculus. J Neurophysiol 85:1673-1685.

Thompson KG, Biscoe KL, Sato TR (2005) Neuronal basis of covert spatial attention in the frontal eye field. J Neurosci 25:9479-9487.

Thompson KG, Hanes DP, Bichot NP, Schall JD (1996) Perceptual and motor processing stages identified in the activity of macaque frontal eye field neurons during visual search. J Neurophysiol 76:4040-4055.

Usher M, McClelland JL (2001) The time course of perceptual choice: the leaky, competing accumulator model. Psychol Rev 108:550-592.

Walton MM, Gandhi NJ (2006) Behavioral evaluation of movement cancellation. J Neurophysiol 96:2011-2024.

948 Wurtz RH, Sommer MA, Paré M, Ferraina S (2001) Signal transformations from cerebral cortex to
949 superior colliculus for the generation of saccades. Vision Res 41:3399-3412.
950 Zandbelt B, Purcell BA, Palmeri TJ, Logan GD, Schall JD (2014) Response times from ensembles of
951 accumulators. Proceedings of the National Academy of Sciences of the United States of America
952 111:2848-2853.

953